# Stormwater runoff microplastics: polymer types,

# particle size, and factors controlling loading rates

Lilia Ochoa<sup>1</sup>, Julianne Chan<sup>1</sup>, Caitlyn Auguste<sup>2</sup>, Georgia Arbuckle Keil, Ph.D.,<sup>2</sup> N.L. Fahrenfeld,

5 Ph.D.<sup>1</sup>

<sup>1</sup>Department of Civil & Environmental Engineering, Rutgers, The State University of New Jersey

<sup>2</sup>Department of Chemistry Rutgers University, Camden, NJ

## **Abstract**

Stormwater runoff is a pathway of entry for microplastics (MPs, plastics <5mm) into aquatic ecosystems. The objectives of this study were to determine MP size, morphology, chemical composition, and loading across urban storm events. Particles were extracted from stormwater samples collected at outfall locations using wet peroxide oxidation and cellulose digestion followed by analysis via attenuated total reflectance (ATR) FTIR. Concentrations observed were  $0.99 \pm 1.10$  MP/L for  $500\text{-}1000~\mu\text{m}$  and  $0.41\pm0.30$  MP/L for the  $1000\text{-}5000~\mu\text{m}$  size ranges. Seventeen different polymer types were observed. MP particle sizes measured using a FTIR-microscope camera indicated non-target size particles based on sieve-size classification, highlighting a potential source of error in studies reporting concentration by size class. A maximum MP load of 38.3 MP/m² of upstream catchment was calculated. MP loadings had moderate correlations with both rainfall accumulation and intensity (Kendall  $\tau = 0.54$  and 0.42, respectively, both p  $\leq 0.005$ ). First flush (i.e. rapid wash-off of pollutants from watershed

- surfaces during rainfall early stages) was not always observed, and antecedent dry days were not
- correlated with MP abundance, likely due to the short dry periods between sampling events.
- Overall, the results presented provide data for risk assessment and mitigation strategies.

## 26 Keywords

Microplastics; Cellulose digestion; Stormwater runoff; Rainfall; Polymers; FTIR

#### Introduction

An estimated 4.8-12.7 million metric tons (MMT) of plastic enter the ocean annually (Wayman and Niemann 2021) and stormwater is an important pathway of entry for microplastics (MPs, plastics <5mm) into the aquatic environment. In fact, it was estimated that stormwater is the source of about 300 times more MPs than wastewater treatment plants in the San Francisco Bay (Sutton, et al. 2019). Land use and climate can influence the characteristics of polymers entering the environment via stormwater runoff. As rainfall increases, the erosive impact of surface runoff rises proportionally, resulting in more transport of plastic debris (Bond, et al. 2022, Sun, et al. 2023, Wei, et al. 2023). Industry, commerce, and transportation activities have been proposed as primary contributors to the prevalence of MPs in urban stormwater runoff (Liu, et al. 2019, Piñon-Colin, et al. 2020, Werbowski, et al. 2021).

MP has been documented in stormwater from around the world including studies in North America (Ross, et al. 2023, Boni, et.al. 2022, Smyth, et al. 2021), Europe (Dris, et al.

2018, Liu, et al. 2019, Lange, et al. 2021), Australia (Herath, et al. 2022, Monira, et al. 2022), and Asia (Sang, et al. 2021, Yano, et al. 2021, Cho, et al. 2023, Xue, et al. 2023). However, making direct comparisons between research data can be challenging due to the differences in the sample collection and stormwater MP extraction procedures that could influence the reported

abundance. Grab (Ziajahromi, et al. 2020, Sang, et al. 2021) or composite (Piñon-Colin, et al.

2020, Boni, et al. 2022), stormwater sampling has been performed usually with relatively small samples (1-8 L), with only one nearing the ASTM 8332 recommended volume of 1500L for low turbidity samples [i.e., 722-1139 L (Liu, et al. 2019)]. Collecting samples small enough for practical transport to the lab for processing (rather than requiring field sieving recommended by ASTM 8332) but large enough to reduce the potential bias introduced by undersized samples is desirable. Many early studies used the method recommended by NOAA (NOAA 2015) for analyzing MP in water samples including a step for NaCl ( $\rho = 1.2$  g/ml) density separation. Density separation is useful for removing some non-target particles (e.g., quartz sand) but biases MP results towards polymers with a density less than or equal to 1.2 g/ml, which does include the most highly manufactured polymers: polyethylene (PE) and polypropylene (PP). The use of high-density solutions such as zinc chloride (ZnCl<sub>2</sub>,  $\rho = 1.8$  g/ml) (Liu, et al. 2019), sodium iodide (NaI,  $\rho = 1.7$  g/ml) (Sang, et al. 2021), lithium metatungstate (LMT,  $\rho = 1.6$  g/ml) (Cho, et al. 2023), and calcium chloride (CaCl<sub>2</sub>,  $\rho = 1.4$  g/ml) (Werbowski, et al. 2021) can improve the capture of denser polymers, including polyvinyl chloride (PVC), polymethyl methacrylate (PMMA), alkyd, polyacrylamide (PAM), polyethylene terephthalate (PET), and polyurethane (PU). This not only captures more polymer types, but also includes some of the polymer types that may be more hazardous (Lithner, et.al. 2011). Ensuring accurate and comparable assessments of microplastic prevalence in urban stormwater runoff requires harmonizing methodologies across investigations. ASTM D8333 provides guidelines for sample preparation from waters and wastewaters for analysis of MPs

(ASTM International 2020). The method includes peroxide digestion (without heat) and cellulose

digestion, and lipase/proteinase digestions to minimize the presence of non-plastic debris, all

46

47

48

49

50

51

52

53

54

55

56

57

58

59

60

61

62

63

64

65

66

67

without the need for density separation. To the author's knowledge, results from stormwater runoff analysis following use of this extraction technique have yet to be reported in the literature.

Therefore, the objectives of this study were to (1) determine the concentration of microplastics (500-5000 µm) in urban stormwater runoff following extraction via ASTM 8333, (2) identify the size, morphology, and chemical composition of the polymers, and (3) calculate MP loading and understand potentially controlling factors (e.g., rainfall intensity). The results presented may help inform treatment and management approaches to mitigate the discharge of microplastics into aquatic environments.

#### **Materials and Methods**

## Sampling

Stormwater runoff sampling was performed during nine different rainfall events from November 2021 to September 2022, at eight stormwater outfalls in urban and suburban areas and one bioretention basin outlet in central New Jersey (Fig.1). The sampling sites, including RE (recreational areas), BB (Bioretention basin), and PR (Paved and residential areas), were selected based on their accessibility, and surrounding land use. All locations sampled have separate sanitary sewers. Runoff from these areas enters stormwater pipelines hydraulically connected to the Raritan River which flows to the Raritan Hudson estuary.

All the samples were collected in 1 L bottles (Natural HDPE plastic wide mouth bottles, Nalgene<sup>TM</sup>), which were attached to a sampling pole and lowered into the flow stream every 10 to 20 min during rainfall events to create 2 to 3 separate composite samples of 3-8 L resulting in a total of 10-16 L of stormwater for each event. The first set of samples was composed of individual samples taken in the initial 20-70 min of the sampling event, followed by the second and third sets formed by samples collected in the subsequent 30 to 80 minutes of sampling.

Sampling began at the onset of rain whenever possible or up to 60 min after the rain began. In instances where rainfall started overnight, sampling began at the earliest opportunity the following morning (Table S4). The duration of each sampling event was adjusted based on weather forecasts to ensure the collection of the target volume of at least 10 liters. Sampling extended beyond the target volume if weather conditions allowed. The process concluded either when rainfall ceased or when the target volume was reached, whichever occurred first.

Samples were transported to the laboratory in a cooler and stored at 4 °C until extraction, which generally took place the next day after collection.

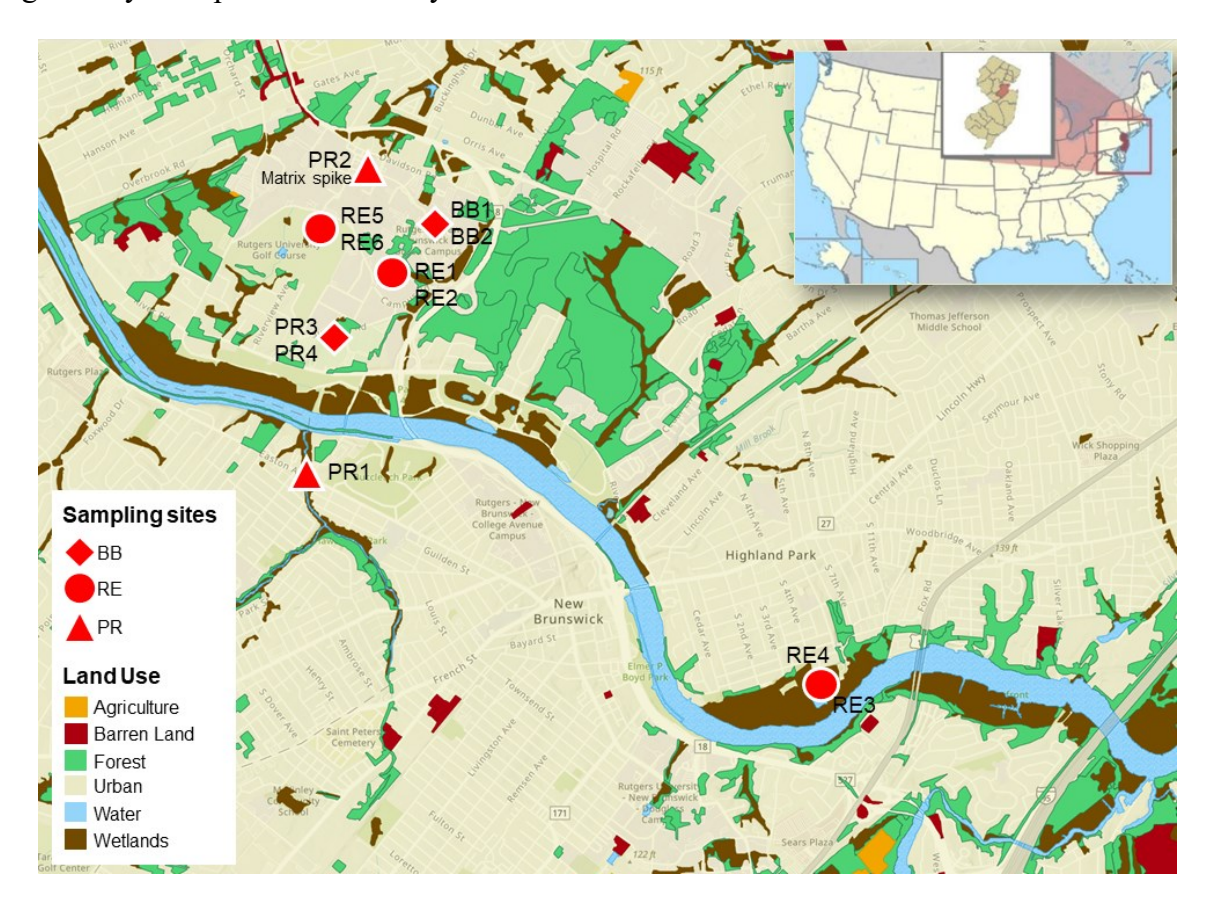


Figure 1. Map of study area showing land use, water bodies, and locations of sampling sites. Insert map shows the location of the study area in central New Jersey, USA, and the location of the state on the US east coast. BB = Bioretention basin, RE = Recreational areas, PR = Paved and residential areas.

For quality assurance and control, field blanks (N=12) were prepared by filling a 1 L bottle with deionized water and leaving it open during the sampling process. These samples were then stored and processed in the same manner as the field samples. The absence of MPs in the field blanks (N=12) within the size range analyzed here (500-5000  $\mu$ m) indicates that the MPs detected in the other samples were not likely the result of contamination during the collection or analysis process. Matrix spikes were performed during one sampling event by adding 20 fragments of red 500  $\mu$ m PP to each 1 L field sample to create two composite sample groups of 5 L. The spiked samples were processed, and the particles were extracted according to the ASTM-D8333 standard method (ASTM International 2020). The extracted particles were transferred onto a glass microscope slide, and the matrix spike PP material was visually identified and counted for the calculation of matrix spike recoveries. The average recovery ( $\pm$  standard error) of matrix spikes was 87.5%  $\pm$  1.06 (N=2).

Table 1. Characteristics of sampled rain events: Sampling date, site, accumulated precipitation, rainfall intensity, antecedent dry days prior to the storm sampling (derived from MRMS (Multi-Radar/Multi-Sensor) precipitation radar data, from the Iowa State University archive - 1-hour data, MultiSensor\_QPE\_01H\_Pass2), estimated runoff, and catchment area.

Rainfall event (y/m/d)	Location	Volume (L)	Accumulated precipitation (mm)	Max rainfall intensity (mm/h)	Antecedent dry days (ADD)	Runoff (mm)	Catchment area (m²)
2021/11/12	BB1	15	12.50	5.40	8	1.03	$7.29 \times 10^2$
2022/3/6	RE1	10	2.60	0.70	2	0.36	$2.87 \times 10^4$
2022/4/6	BB2	11	20.30	3.2	1	4.33	$7.29 \times 10^2$
	RE2	12	20.00	3.2	1	4.90	$2.87 \times 10^4$
2022/5/7	PR1	16	36.50	4.5	0	13.44	$1.49 \times 10^7$
2022/5/19	RE3	12	32.40	8.4	1	10.65	$1.63 \times 10^4$
	RE4	12	32.40	8.4	1	10.65	$1.63 \times 10^4$
2022/6/16	PR2	12	9.60	3	3	1.26	$3.74 \times 10^4$
2022/6/23	PR3	12	3.50	2.3	0	0.17	1.33×10 <sup>5</sup>

Rainfall event (y/m/d)	Location	Volume (L)	Accumulated precipitation (mm)	Max rainfall intensity (mm/h)	Antecedent dry days (ADD)	Runoff (mm)	Catchment area (m²)
	PR4	12	3.50	2.3	0	0.17	$1.33 \times 10^5$
2022/6/27	RE5	12	5.50	2.5	3	0.08	$5.85 \times 10^3$
2022/9/6	RE6	12	21.30	5.8	0	8.36	$5.85 \times 10^3$
2023/7/18	PR2- Matrix spike	10	7.70	5.5	1	0.33	3.74×10 <sup>4</sup>

#### **Microplastics extraction**

First, composite samples were wet-sieved through 1000 µm and 500 µm sieves. The particles of each sieve were transferred to 250 ml glass beakers after being thoroughly rinsed with deionized (DI) water and covered with aluminum foil to prevent contamination (ASTM International 2020). Extraction was performed following ASTM-D8333-20 (ASTM International 2020) with minor modifications. Briefly, wet peroxide oxidation (WPO) was performed using 20 mL of aqueous 0.05 M Fe (II) solution and 20 mL of 30% hydrogen peroxide added to the beakers and heated to 75°C for 30 min to reduce the amount of non-target organic matter in downstream analyses as per the NOAA Method recommendations (NOAA 2015). After cooling down, the material of each beaker was transferred to one or more 50 mL Falcon tubes, depending on the DI water used to transfer the solids content from the sieves to the beakers. The tubes were centrifuged at 5000 rpm (4276×g) for 3 min to pellet particulate matter. Glass pipettes were used to remove as much of the remaining hydrogen peroxide solution supernatant as possible from the tubes without disturbing the pellets.

Next, cellulose digestion was performed via a modified Schweizer's reagent (2.5 g copper (II) hydroxide added to 100 mL of 30% ammonium hydroxide). After adding 40 mL of the modified Schweizer's reagent to each Falcon tube containing the sample pellet, tubes were

placed for 5 min on a laboratory shaker at 50 rpm, then centrifuged for 3 minutes at 5000 rpm (4276×g). The modified Schweizer's reagent supernatant was removed using a disposable glass pipette, again, without disturbing the pellet or removing floating debris. Then, 25 mL of 30 % ammonium hydroxide was added to the centrifuge tubes to solvate any remaining modified Schweizer's reagent, repeating the shaking and centrifugation described above, and the remaining 30% ammonium hydroxide solution was removed from the tubes with a glass pipette. When multiple Falcon tubes were used for the same sample, the contents were combined at the end of the extraction process and re-sieved to finally collect the material on 63  $\mu$ m stainless steel mesh (TWP, Berkeley, CA), which were placed in glass Petri dishes until analysis. Focusing on particles collected on the 500  $\mu$ m sieve and greater allowed for analysis of all particles without subsampling. Note, abundance of total particles remaining post extraction in the smaller size ranges were too numerous for analysis without subsampling with average  $\pm$  standard deviation of  $138 \pm 102$  particles in the 300-500  $\mu$ m,  $209 \pm 240$  particles in the 150-300  $\mu$ m  $504 \pm 409$  particles in the 63-150  $\mu$ m size ranges.

## Spectral analysis

Attenuated Total Reflectance Fourier Transform Infrared (ATR-FTIR) Spectroscopy was performed on all particles >500 µm (N=643 particles) using a Bruker Alpha spectrometer, equipped with a single-bounce diamond internal reflection element (IRE) ATR accessory. Prior to the spectral acquisition, visual characteristics, including the color and morphology of each particle were documented. The morphologies of particles were classified as beads (i.e., spheres), fragments, films, and fibers/rods (example images are included in Fig. S1). Particles were transferred to the Alpha ATR-FTIR spectrometer using metal tweezers or a paintbrush. Spectral data were collected by conducting 32 scans per particle at a resolution of 4 cm<sup>-1</sup> within a

wavenumber range of 4000 to 400 cm<sup>-1</sup>. Background scans of air were performed before data collection and periodically during analysis using the same number of scans, resolution, and wave number range to facilitate background correction of environmental particle spectra.

Spectra were analyzed using OpenSpecy, which employs a Pearson correlation between the reference spectra and the test spectrum for matching (Cowger, et al. 2021). For each particle, the top five polymer matches and their respective match coefficient were recorded, followed by manual confirmation of the spectral bands against reference spectra to establish the polymer type. Generally, particles that scored over 0.5 match (i.e., Pearson correlation coefficient) with a consistent polymer were classified as microplastic matched to that polymer type.

A FTIR-microscope camera (8x Cassegrain-Objective, Bruker LUMOS II spectrometer, Bruker Optics, Billerica, MA) was used to determine the length of the longest axis for particles classified as microplastic using the measuring tool available in OPUS 7.8 (Bruker Optics, Billerica, MA). For fibers that were not knotted, this corresponded to the full fiber length; for knotted fibers, this was reported as the total length of knotted bundle for practicality.

Measurement was conducted for all particles that remained intact after the ATR-FTIR analysis.

#### Rainfall characteristics and runoff

Based on data captured by MRMS (Multi-Radar/Multi-Sensor) precipitation radar data from the Iowa State University archive (1-hr data, MultiSensor\_QPE\_01H\_Pass2, https://mtarchive.geol.iastate.edu) it was possible to estimate the accumulated precipitation and rainfall intensity during each sampling event (Table1). Watersheds associated with the sampling locations were delineated by mapping the anticipated flow direction of overland runoff using a Digital Elevation Model (DEM) (https://apps.nationalmap.gov/downloader/) to calculate the contributing drainage area (ESRI ArcGIS Pro 3.2, 2023. Redlands, CA: Environmental Systems

Research Institute) and assess the influence of catchment characteristics on microplastic abundance. Subsequently, the direct surface runoff from the rainfall events of interest was estimated through the Soil Conservation Service—Curve Number (SCS-CN) method by integrating the DEM to land use/land cover and soil data, which were obtained from the MRLC (https://www.mrlc.gov) and SSURGO datasets (https://www.nrcs.usda.gov/resources/data-and-reports/soil-survey-geographic-database-ssurgo), respectively. Processing was performed using ArcHydro Tools for ArcGIS Pro 3.2. Finally, microplastic loads in stormwater runoff were calculated based on the following equation (Piñon-Colin, et al. 2020):

$$L = C \times \frac{1000L}{1m^3} \times Q \times \frac{1m}{1000mm} = C \times Q$$

where L is MP load [MP/m<sup>2</sup>], C is MP concentration [MP/L], Q is runoff [mm]

## Statistical analysis

All statistical analyses were performed using R (v4.1.2) and the vegan package (https://cran.r-project.org/web/packages/vegan/) and/or Excel 2016 (Microsoft, USA). Non-normality of data was confirmed with a Shapiro-Wilk test. A Kruskal-Wallis test was used to compare the difference in the microplastic concentrations among the first, second, and third composite sample groups followed by a post hoc Dunn test. A paired Wilcoxon rank sum test was used to compare the microplastic concentrations between the two size classes (1000-5000 μm and 500-1000 μm). A Kendall's tau test evaluated correlations between microplastic load and accumulated precipitation. Associations between microplastic load and antecedent dry days, as well as microplastic load and rainfall intensity, were examined using the same test. A chi-square test was used to examine the correlation between the morphology and size class, and morphology and polymer type. Shannon indices were calculated to compare the richness of polymers across

sampling locations and analyzed as a function of storm, land use, and size class via PERMANOVA. Finally, non-metric multidimensional scaling (nMDS) was used to visually represent polymer profiles and assess the similarities between sampling sites, composite sample groups, and accumulated precipitation. Figures and statistics were based on the actual particle size (i.e. the length of the longest measured axis of the MP), with particles reassigned as needed to a larger or smaller sieve size range. The significance level was set to 0.05 in all cases.

#### **Results**

## Polymers and morphologies observed

A total of 207 particles (32.19%, total N=643) in the stormwater samples within the 500-5000 μm size range were identified as MPs (Fig. 2). The analysis revealed 17 polymer types in stormwater including the presence of both positively (ρ ≤1.1 g cm<sup>-3</sup>) and negatively buoyant polymers (ρ >1.1 g cm<sup>-3</sup>), based on standard densities from Table S1. Example spectra are included in Fig. S2a to Fig. S2d. Out of the 207 MPs observed, buoyant polymer groups identified included polyethylene, which was the most commonly observed polymer (N=75 PE). Other positively buoyant polymers identified included polystyrene (N=20 PS), polypropylene (N=20 PP), polydimethylsiloxane (N=6 PDMS), synthetic resin (N=5), and ethylene propylene rubber (N=1 EPM). Positively buoyant polymers constituted 61.35% of the total abundance of MP in this study. Negatively buoyant polymer types included polyvinyl chloride (N=20 PVC), polyurethane (N=14 PU), polyacrylamide (N=11 PAM), aramid (N=9), polyamide (N=7 PA), polychloroprene (N=5 CR), polyethylene terephthalate (N=5 PET), alkyd varnish (N=5), polymethyl methacrylate (N=2 PMMA), polyvinyl alcohol (N=1 PVA), and polysulfone (N=1 PSU) representing 38.64% of all stormwater microplastics.

As anticipated, some of these particles exhibited surface oxidation in their spectra indicative of environmental weathering, identified by the presence of a hydroxyl (OH) band, typically observed in the region of 3000-3600 cm<sup>-1</sup> in the spectra (Fig. S4).

Particles that were not MP (out of total N=643 total particles analyzed) were identified as cellulosic material, such as cellulosic fibers (cotton, flax, linen), cellulose, and leaf plant (26.13%); matter from biota, including crangon, and chitin (14%); other materials, such as brood comb, coal, and quartz (7.16%); and unidentified particles (20.52%) (Fig. S5).

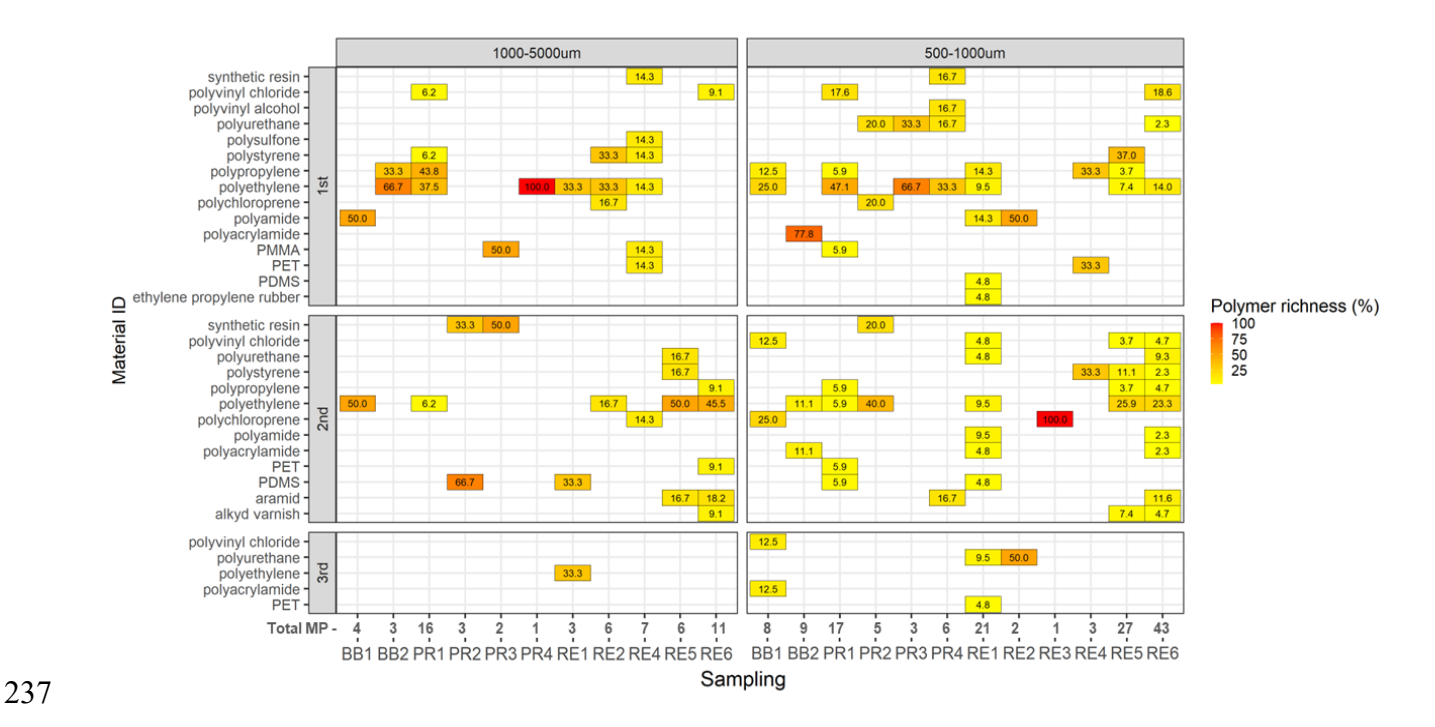


Figure 2. Heatmap showing the distribution of polymer types as a percentage of MPs found in the sampling events, rounded to one decimal point, with polymer diversity represented by horizontal blocks within the composite sample groups ( $1^{st}$ ,  $2^{nd}$ , and  $3^{rd}$ ), and particle size categories by vertical blocks. (PET= polyethylene terephthalate, PMMA= polymethyl methacrylate, PDMS= polydimethylsiloxane).

MPs 500-5000 μm had an average length (± standard deviation) of 1552±1462 μm (N=117/207 MPs total) for their longest dimension. Particles with their longest dimension smaller than the sieve size were observed. Histograms depicting the longest measured dimension across various particle morphologies demonstrated right-skewed data (Fig.3). Fragments were the most commonly observed MP morphology followed by films. The occurrence of beads (i.e., spheres) and rod-fibers was infrequent.

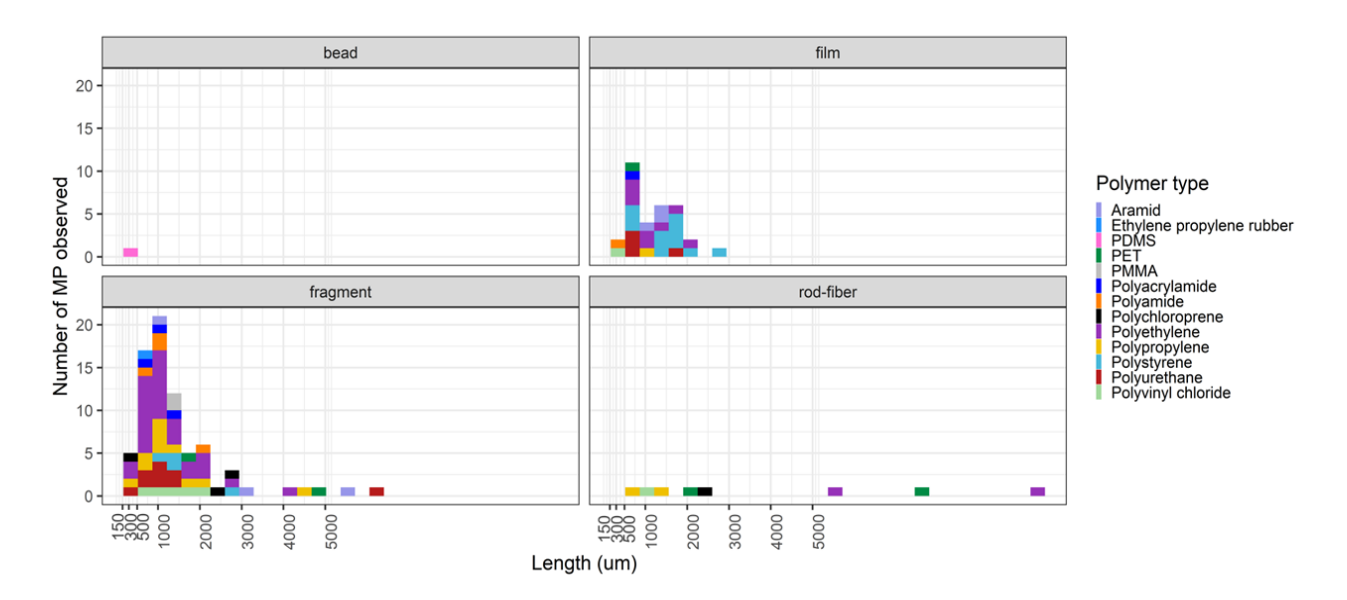


Figure 3. Histograms displaying the measured particle length (N=117/207 MPs total) categorized by particle morphology and color-coded by observed particle polymer. Natural and unknown materials have been excluded from the analysis.

The polymer profiles visualized via nMDS resulted in no distinct clustering by size class, sampling location, composite sample groups, or cumulative precipitation (Fig. S6). Likewise, the outcomes of the chi-square test of independence indicate that there is no statistically significant association between the size category and polymer type ( $\chi^2 = 7.31$ , p = 0.06), nor between morphology and polymer ( $\chi^2 = 14.234$ , p = 0.286). Shannon diversity indices calculated for polymers in the 500-1000  $\mu$ m or 1000-5000  $\mu$ m size ranges for a given site and storm event

ranged from zero to 2.0 (average  $\pm$  standard deviation 1.0  $\pm$  0.6, Fig. S7). No differences were seen by size class, storm event, or land use (all p>0.46, PERMANOVA).

## **Microplastics concentration**

MPs were observed in all samples within the 500-1000 μm size range and in 11 out of 12 samples in the 1000-5000 μm size range. The average of total MP concentration (± standard deviation) was 1.40±1.29 MP/L with a maximum of 4.58 MP/L observed during sampling at RE6 (Fig. 4). Significantly greater total MP concentrations were observed in the smaller size class (500-1000 μm) having an average of 0.99±1.10 MP/L compared to the larger size class (1000-5000 μm) having an average of 0.41±0.30 MP/L (p=0.03, paired Wilcoxon). There were no significant differences in the microplastic concentrations comparing the first-second (p=0.74), second-third (p=0.54), and first-third (p=0.73) composite samples including all storm events (Fig. 4; Kruskal-Wallis p=0.43). Of the twelve sampling events, samples were collected at the onset of precipitation for six sampling events (BB1, RE1, RE3, RE4, PR2, RE5). In three of these events (BB1, RE1, RE4), the first composite sample had a higher concentration of MP.

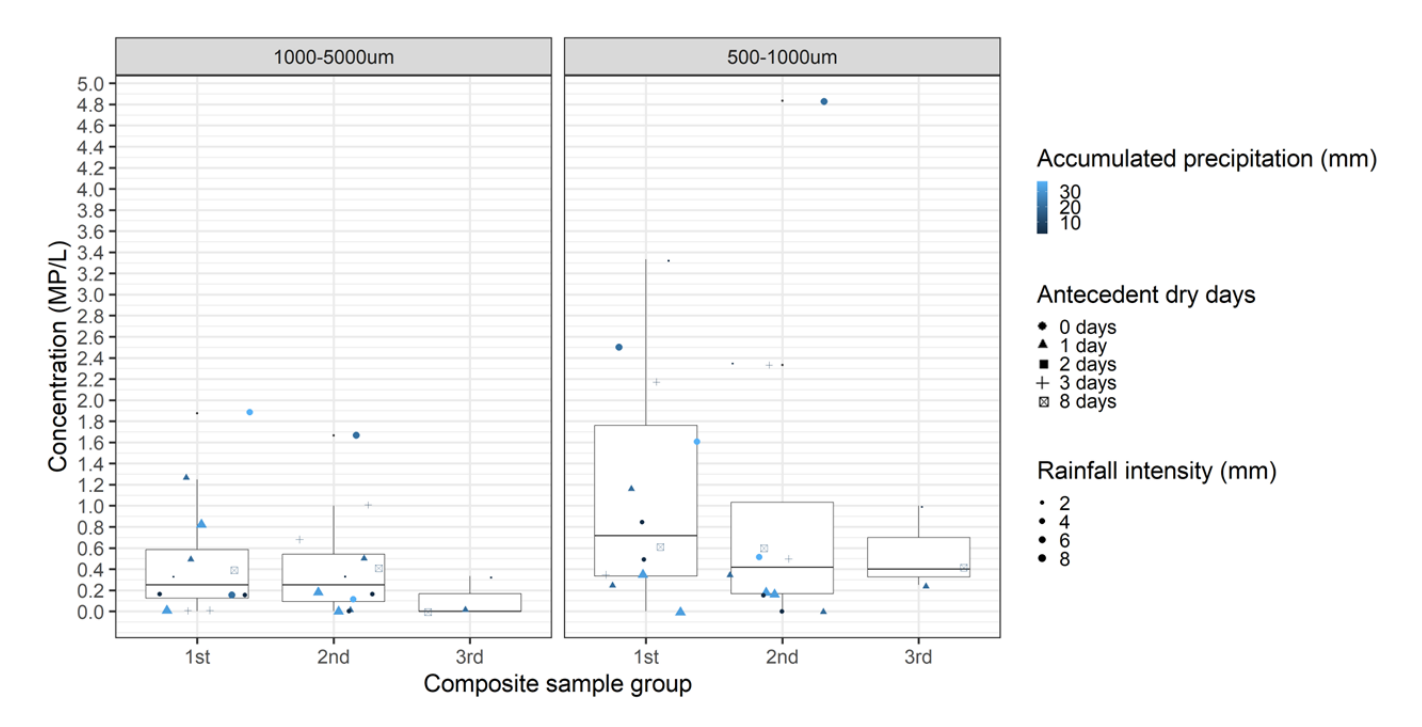


Figure 4. Boxplots of MP concentrations (MP particles per liter of water) observed in the 1000-5000 µm and 500-1000 µm size class, which were divided into composite samples. The first group of samples represents the concentration found during the initial 20 to 70 minutes of the sampling events, followed by the second and third groups (30 to 80 minutes). Symbols for the jitter plot correspond to the antecedent dry days, the size for the jitter corresponds to the rainfall intensity, and the color to the accumulated precipitation observed during the storm event.

## Microplastic load

The highest microplastic load (38.3 MP/m²) (Fig.5) was observed at RE6, on a golf course that collects stormwater mainly from grassy areas and parking lots. The second highest load was in the PR1 site with 27.7 MP/m², a manhole that discharged stormwater from residential areas and paved streets into the Mile Run, a tributary of the Millstone River. The results of Kendall's tau test indicated a moderate positive relationship between the estimated microplastic load and accumulated precipitation ( $\tau = 0.54$ , p =1.4x10<sup>-4</sup>) as well as between the microplastic

load and rainfall intensity during samplings ( $\tau$  = 0.42, p =0.005). Conversely, no significant correlation was found between antecedent dry days and the estimated MP load per site ( $\tau$  = -0.24 p = 0.13).

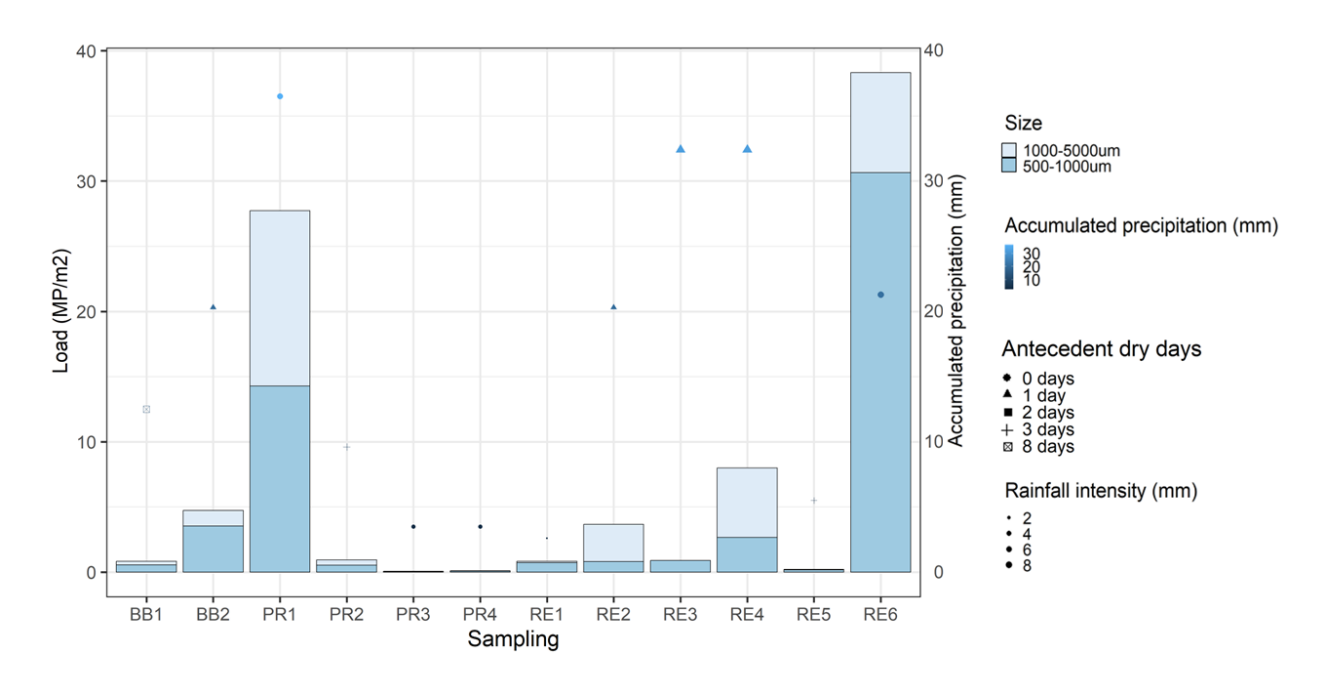


Figure 5. MP load (MP/m²) in stormwater was observed for particles of 1000-5000 µm and 500-1000 µm size class. Symbols for the jitter plot correspond to the antecedent dry days, the size correspond to the rainfall intensity and color to the accumulated precipitation observed during the storm event.

## Discussion

## Polymer types and particle morphologies in stormwater

The most prevalent polymers in this study were PE (36.23%), PP (9.66%), and PS (9.66%), which are consistently reported across the stormwater literature (Shruti, et al. 2021), and previously were reported as the majority in NJ stormwater (Bailey, et al. 2021, Boni, et al. 2022, Parmar, et al. 2023). The dominance of these plastic types corresponded with these materials being the most highly manufactured (Plastics Europe 2022) and is likely also attributed

to their widespread use in everyday items. The polymer richness (i.e., number of unique polymer types) in this study at the points where BR1, BR2, RE1, and RE2 samplings were carried out, was greater (EPM, PDMS, PET, PAM, PA, CR, PE, PP, PS, PU, PVC, 500-5000µm) compared to previous work from our team performed in the same sampling points and similar size range (PE, PS, PP, copolymer of ethylene-ethyl acrylate (COPOLY), PET, and acrylonitrile styrenebutadiene (ABS, 250-2000µm) but using NaCl density separation (Boni et al. 2022). It is difficult to say whether this is because denser particles were retained in the samples from this study by not using density separation (although some denser than expected particles were previously observed), more locations were sampled in the present study (nine versus three), the collection of greater sample volumes (12-15 L vs. 5 L), or due to other spatiotemporal differences. Other stormwater investigations that did not perform density separation (Table S2) reported approximately half of the MPs in stormwater were non-buoyant polymers ( $\rho > 1.1 \text{ g/cm}^{-1}$ <sup>3</sup>). For instance, Ross et al. (2023) found that, for particle sizes ranging from 500 to 1000 μm, 60% of the polymer profile consisted of non-buoyant polymers. Similarly, studies examining smaller size classes (e.g., 100-5000 μm, 15-1820 μm, 54-1000 μm) without density separation reported an approximate 50% prevalence of non-buoyant polymers (Mak, et al. 2020, Sang, et al. 2021, Monira, et al. 2022). In contrast, earlier studies performing density separation with NaCl  $(\rho = 1.2 \text{ g/ml})$  reported varying percentages of non-buoyant polymers, ranging from 33% to 50% (Piñon-Colin, et al. 2020, Yano, et al. 2021, Herath, et al. 2022, Boni et al. 2022, Xue, et al. 2023). Some of these negatively buoyant polymers are of potential interest given a hazard ranking model, where polymers such as PU and PVC are classified as toxic and carcinogenic to humans (Lithner, et al. 2011). Both of these polymers were observed in the present study and in

302

303

304

305

306

307

308

309

310

311

312

313

314

315

316

317

318

319

320

321

322

other stormwater studies (Liu, et al. 2019, Sang, et al. 2021, Werbowski, et al. 2021, Cho, et al. 2023, Parmar, et al. 2023, Xue, et al. 2023).

During the spectral characterization through ATR-FTIR, analysis proved challenging for certain black particles. All these particles shared the characteristics of being easily crumbled or fragmented (11.50% of N=643 total particles), preventing the acquisition of high-quality spectra. This difficulty may be attributed to the presence of carbon black, as suggested by Rasmussen et al. (2023), who also encountered challenges in particle identification and opted for pyrolysis-gas chromatography-mass spectrometry (Py-GC/MS) instead of FTIR, specifically for identifying tire wear particles.

The polymer morphologies observed in this study were primarily fragments, consistent with some other stormwater studies (Werbowski, et al. 2021, Ashiq, et.al. 2023, Parmar, et al. 2023). Only 15 fibers/rods were observed out of 207 total MPs, potentially because all samples were taken from stormwater outfalls with separate sanitary sewer systems (compared to a study with many fibers in combined sewer, (Piñon-Colin, et al. 2020), or/and unknotted fibers may pass through the sieves. Additionally, a prior (Yurtsever 2021) suggested that cellulose digestion dissolves mixtures of cellulose fibers and plastic microfibers, potentially reducing the fibers observed in the results presented here. Notably, the cellulose digestion (e.g., modified Schweizer's reagent) used to reduce the presence of non-plastic debris resulted in the further fragmentation of natural materials that were not dissolved. Thus, re-sieving of samples was required to remove non-target size debris. Organic matter was still identified in all of our samples including cellulosic fibers and animal matter, which were unlikely to be digested. Therefore, future researchers may consider sieving post-digestion, rather than pre-digestion as

recommended by ASTM 8332, to reduce the number of sample transfers, each introducing a risk of particle loss.

Measuring the length of microplastics rather than relying on sieve size resulted in several instances where the measured particle size was smaller than the expected size based on the sieve used, as we previously noted (Parmar, et al. 2023). This was attributed to the asymmetrical nature of the particles, where different sides may have different dimensions and may pass through or get stuck in different sieves, or/and because they could have initially been in aggregates, or the sieve was partially clogged from other particles of the samples which caused the retention of smaller particles in a bigger size sieve. Reporting actual particle size, as done here, or applying corrections for sieve size misclassifications is recommended for accurate microplastic characterization in stormwater studies. Given ASTM 8332 (ASTM International 2020) is recommended also for destructive analytical techniques (i.e., pyrolysis GC/MS), researchers should carefully consider the expected error in particle size resulting from sieving non-spherical fragments. Direct particle size measurement in addition to reporting particle counts or concentrations as size ranges may also be beneficial for facilitating cross-study comparison, given the lack of harmonized methods (including particle size ranges selected for reporting) in the MPs literature to date.

#### **Microplastics concentration in stormwater**

346

347

348

349

350

351

352

353

354

355

356

357

358

359

360

361

362

363

364

365

366

367

368

The MP concentrations reported in this study (Table S3), ranging from 0.08 to 4.58 MP/L (500-5000 μm), are within the range or greater than others previously reported in the same geographical area (0.30 to 0.90 MP/L (250-2000 μm) (Boni et al. 2022), 0.4 to 0.6 MP/L (2000-5000 μm) (Bailey, et al. 2021). Comparing to sites previously sampled by Boni et al. (2022), concentrations were within one to two orders of magnitude (i.e., 79%-90% RPD) for the site

adjacent to a soccer field (RE1-RE2), and 18.00%-116% RPD for the outlet in the bioretention cell (BB1-BB2)). Likewise, the stormwater MP concentrations were reasonably consistent despite the differences in methods including density separation via NaCl or NaI, but similar range in their size classes: 0.34 to 5.05 MP/L (1000-5000 μm, NaI) from stormwater pipes in China (Sang, et al. 2021), 0.30 to 17.3 MP/L (300-5000 μm, NaCl) from roadside rainwater draining pits in Thailand (Xue, et al. 2023), and 1.9 to 2.46 MP/L (48.5-2500 μm, NaCl) from retention ponds in Australia (Herath, et al. 2022). As others have noted, MP count-based concentrations were greater in smaller sizes classes (Grbic, et al. 2020, Parmar, et al. 2023, Järlskog, et al. 2020, Cho, et al. 2023).

## Environmental factors potentially controlling microplastic load

MP in stormwater runoff have predominantly been reported as the number of MPs per volume. However, several factors potentially control microplastic abundance including land use, watershed characteristics, drainage systems, and precipitation characteristics such as antecedent dry days, accumulated precipitation, and rainfall intensity (Mamun, et al. 2020, Chen, et al. 2023) that can be difficult to disentangle in field studies like this, but are important to take into account meaning that two samples with the same concentration are likely to contain different amounts of MPs. Despite the importance of these considerations, there is currently a limited number of studies reporting on microplastic load in stormwater runoff (MP/m²) (Piñon-Colin, et al. 2020, Cho, et al. 2023). In this study, with respect to land use, the highest total MP loads were observed at an outfall located on a golf course, adjacent to moderately trafficked roads and parking lots (RE6) and the second highest in a dense residential area (PR1). Others (Zhou, et al. 2021, Cho, et al. 2023) have reported that impervious surfaces such as industrial catchment areas or paved areas exacerbate stormwater runoff and the amount of MP released into the

environment. MPs and other pollutants are therefore more likely to be transferred to receiving water after washing off these impermeable surfaces. Comparing samples collected at the same location during different rainfall events indicated that greater microplastic loading occurred during more intense rainfall events, e.g., (Cho, et al. 2023).

The lack of relationship between microplastic loading and antecedent dry days was likely because of the relatively short number of antecedent dry days prior to sampling, preventing the accumulation of deposited plastics. Other teams that did observe a relationship between these variables had longer periods between wet weather events, with the maximum dry days ranging from 11 to 183 (Piñon-Colin, et al. 2020, Smyth, et al. 2021, Cho, et al. 2023). The absence of a pronounced first flush across samples collected at the onset of precipitation in our study, a phenomenon well documented for other pollutants (e.g., Luo et al., 2009), may be attributed to the timing of sampling and/or decisions about sample pooling potentially resulting in dilution of samples with higher concentrations. The short number of antecedent dry days may also result in lower load in the first-flush, Sun et al. (2023) did not detect a MP first flush during a storm event preceded by 8 antecedent dry days (the longest antecedent dry day period in this study) but did observe a first flush during their sampling event with the highest rainfall intensity (10.56 mm/h).

#### **Conclusion**

Urban stormwater runoff samples extracted using a modified ASTM 8333 extraction, including cellulose digestion, had a greater polymer richness but reasonably consistent count-based concentrations compared to our previous work that used different extraction techniques (with density separation, without cellulose digestion) and sampled smaller volumes of water (Bailey, et al. 2021, Boni et al. 2022). While larger sample volumes are expected to capture a greater diversity of polymer types than undersized sample volumes (Parmar, et al. 2023) as is

using extraction techniques that capture denser particles (either by not performing density separation or by using denser solutions (Shruti, et al. 2021), direct comparison of the impacts of cellulose digestion remains to be reported to the authors' knowledge. Notably, in treatment with the Schweizer reagent, samples needed to be re-sieved to eliminate non-target size and (presumably) non-microplastic debris, which could reduce the workload for analytical methods that require particle-by-particle analysis. This, of course, assumes that target materials were not fragmented or dissolved, while as noted above, the cellulose digestion could remove some fibers, resulting in an underestimation of microplastic concentrations. The relationship between microplastic loads and rainfall characteristics (rainfall intensity and accumulated precipitation) was confirmed, but being able to sample in a period with a greater number of antecedent dry days may be needed to capture relationships demonstrated in other catchments (e.g., first flush phenomena). Besides the quantification of MP concentration, the direct measurement of the particle size, morphology, chemical composition can provide valuable inputs for assessing potential environmental hazards particularly given that these characteristics influence ingestion by biota (Ma, et al. 2020).

430

431

432

433

434

415

416

417

418

419

420

421

422

423

424

425

426

427

428

429

## Acknowledgments

Funding for the project was provided by Water Research Foundation 5088 and National Science Foundation Grant 1917676. LO was supported by a Mark B. Bain Fellowship from the Hudson River Foundation.

435

436

- 1. Ashiq, M. M., Jazaei, F., Bell, K., Ali, A. S. A., Bakhshaee, A., & Babakhani, P. (2023).
- Abundance, spatial distribution, and physical characteristics of microplastics in
- stormwater detention ponds. Frontiers of Environmental Science & Engineering, 17(10).
- 443 doi:10.1007/s11783-023-1724-y
- 2. ASTM International. 2020. "D8332. Standard practice for collection of water samples
- with high, medium, or low suspended solids for identification and quantification of
- 446 microplastic particles and fibers."
- 3. ASTM International. 2020. "D8333. Standard practice for preparation of water samples
- with high, medium, or low suspended solids for identification and quantification of
- 449 microplastic particles and fibers using Raman spectroscopy, IR spectroscopy, or
- 450 Pyrolysis-GC/MS."
- 4. Bailey, K., Sipps, K., Saba, G. K., Arbuckle-Keil, G., Chant, R. J., & Fahrenfeld, N. L.
- 452 (2021). Quantification and composition of microplastics in the Raritan Hudson Estuary:
- Comparison to pathways of entry and implications for fate. *Chemosphere*, 272(129886),
- 454 129886. doi:10.1016/j.chemosphere.2021.129886
- 5. Bond, C., Li, H., & Rate, A. W. (2022). Land use pattern affects microplastic
- 456 concentrations in stormwater drains in urban catchments in Perth, Western Australia.
- 457 Land, 11(10), 1815. doi:10.3390/land11101815
- 6. Boni, W., Arbuckle-Keil, G., & Fahrenfeld, N. L. (2022). Inter-storm variation in
- 459 microplastic concentration and polymer type at stormwater outfalls and a bioretention

- basin. The Science of the Total Environment, 809(151104), 151104.
- 461 doi:10.1016/j.scitotenv.2021.151104
- 462 7. Chauhan, J. S., Semwal, D., Nainwal, M., Badola, N., & Thapliyal, P. (2021).
- Investigation of microplastic pollution in river Alaknanda stretch of Uttarakhand.
- Environment Development and Sustainability, 23(11), 16819–16833.
- 465 doi:10.1007/s10668-021-01388-y
- 8. Chen, Y., Niu, J., Xu, D., Zhang, M., Sun, K., & Gao, B. (2023). Wet deposition of
- globally transportable microplastics (<25 µm) hovering over the megacity of Beijing.
- 468 Environmental Science & Technology, 57(30), 11152–11162.
- 469 doi:10.1021/acs.est.3c03474
- 470 9. Cho, Y., Shim, W. J., Ha, S. Y., Han, G. M., Jang, M., & Hong, S. H. (2023).
- 471 Microplastic emission characteristics of stormwater runoff in an urban area: Intra-event
- variability and influencing factors. *The Science of the Total Environment*, 866(161318),
- 473 161318. doi:10.1016/j.scitotenv.2022.161318
- 10. Cowger, W., Steinmetz, Z., Gray, A., Munno, K., Lynch, J., Hapich, H., ... Herodotou,
- O. (2021). Microplastic spectral classification needs an open source community: Open
- Specy to the rescue! *Analytical Chemistry*, 93(21), 7543–7548.
- 477 doi:10.1021/acs.analchem.1c00123
- 11. Dris, Rachid, Johny Gasperi, and Bruno Tassin. 2018. "Sources and fate of microplastics
- in urban areas: a focus on Paris megacity." Freshwater Microplastics. The Handbook of
- 480 Environmental Chemistry, 69-83.

- 481 12. Estahbanati, S., & Fahrenfeld, N. L. (2016). Influence of wastewater treatment plant
- discharges on microplastic concentrations in surface water. *Chemosphere*, 162, 277–284.
- 483 doi:10.1016/j.chemosphere.2016.07.083
- 484 13. Grbić, J., Helm, P., Athey, S., & Rochman, C. M. (2020). Microplastics entering
- 485 northwestern Lake Ontario are diverse and linked to urban sources. *Water Research*,
- 486 174(115623), 115623. doi:10.1016/j.watres.2020.115623
- 487 14. Herath, S., Hagare, D., Siddiqui, Z., & Maheshwari, B. (2022). Microplastics in urban
- stormwater-developing a methodology for its monitoring. Environmental Monitoring and
- 489 Assessment, 194(3), 173. doi:10.1007/s10661-022-09849-1
- 490 15. Hu, Y., Gong, M., Wang, J., & Bassi, A. (2019). Current research trends on microplastic
- 491 pollution from wastewater systems: a critical review. *Re/Views in Environmental Science*
- 492 and Bio/Technology, 18(2), 207–230. doi:10.1007/s11157-019-09498-w
- 16. Järlskog, I., Strömvall, A.-M., Magnusson, K., Gustafsson, M., Polukarova, M., Galfi, H.,
- 494 ... Andersson-Sköld, Y. (2020). Occurrence of tire and bitumen wear microplastics on
- 495 urban streets and in sweepsand and washwater. The Science of the Total Environment,
- 496 729(138950), 138950. doi:10.1016/j.scitotenv.2020.138950
- 497 17. Lange, K., Magnusson, K., Viklander, M., & Blecken, G.-T. (2021). Removal of rubber,
- bitumen and other microplastic particles from stormwater by a gross pollutant trap -
- bioretention treatment train. Water Research, 202(117457), 117457.
- 500 doi:10.1016/j.watres.2021.117457
- 18. Lithner, D., Larsson, A., & Dave, G. (2011). Environmental and health hazard ranking
- and assessment of plastic polymers based on chemical composition. The Science of the
- 503 Total Environment, 409(18), 3309–3324. doi:10.1016/j.scitotenv.2011.04.038

- 19. Liu, F., Olesen, K. B., Borregaard, A. R., & Vollertsen, J. (2019). Microplastics in urban
- and highway stormwater retention ponds. The Science of the Total Environment, 671,
- 506 992–1000. doi:10.1016/j.scitotenv.2019.03.416
- 507 20. Luo, H., Luo, L., Huang, G., Liu, P., Li, J., Hu, S., ... Huang, X. (2009). Total pollution
- effect of urban surface runoff. Journal of Environmental Sciences (China), 21(9), 1186–
- 509 1193. doi:10.1016/s1001-0742(08)62402-x
- 510 21. Ma, H., Pu, S., Liu, S., Bai, Y., Mandal, S., & Xing, B. (2020). Microplastics in aquatic
- environments: Toxicity to trigger ecological consequences. Environmental Pollution
- 512 (Barking, Essex: 1987), 261(114089), 114089. doi:10.1016/j.envpol.2020.114089
- 513 22. Mak, C. W., Tsang, Y. Y., Leung, M. M.-L., Fang, J. K.-H., & Chan, K. M. (2020).
- Microplastics from effluents of sewage treatment works and stormwater discharging into
- the Victoria Harbor, Hong Kong. Marine Pollution Bulletin, 157(111181), 111181.
- 516 doi:10.1016/j.marpolbul.2020.111181
- 517 23. Mamun, A. A., Shams, S., & Nuruzzaman, M. (2020). Review on uncertainty of the first-
- flush phenomenon in diffuse pollution control. *Applied Water Science*, 10(1).
- 519 doi:10.1007/s13201-019-1127-1
- 520 24. Maniquiz-Redillas, M., Robles, M. E., Cruz, G., Reyes, N. J., & Kim, L.-H. (2022). First
- flush stormwater runoff in urban catchments: A bibliometric and comprehensive review.
- 522 *Hydrology*, 9(4), 63. doi:10.3390/hydrology9040063
- 523 25. Monira, S., Roychand, R., Bhuiyan, M. A., Hai, F. I., & Pramanik, B. K. (2022).
- Identification, classification and quantification of microplastics in road dust and
- stormwater. *Chemosphere*, 299(134389), 134389.
- 526 doi:10.1016/j.chemosphere.2022.134389

- 527 26. NOAA. 2015. "Laboratory Methods for the Analysis of Microplastics in the Marine
- Environment." *NOAA Marine Debris Program* 1-29.
- 529 27. Parmar, S., Arbuckle-Keil, G., Kumi, G., & Fahrenfeld, N. L. (2023). Urban stormwater
- microplastic size distribution and impact of subsampling on polymer diversity.
- Environmental Science. Processes & Impacts, 25(8), 1374–1384.
- 532 doi:10.1039/d3em00172e
- 533 28. Piñon-Colin, T. de J., Rodriguez-Jimenez, R., Rogel-Hernandez, E., Alvarez-Andrade,
- A., & Wakida, F. T. (2020). Microplastics in stormwater runoff in a semiarid region,
- Tijuana, Mexico. The Science of the Total Environment, 704(135411), 135411.
- doi:10.1016/j.scitotenv.2019.135411
- 537 29. Plastics Europe. 2022. *Plastics- the Facts 2022*. Annual Report, Brussels: Plastics Europe
- 538 AISBL.
- 30. Rasmussen, L. A., Lykkemark, J., Andersen, T. R., & Vollertsen, J. (2023). Permeable
- pavements: A possible sink for tyre wear particles and other microplastics? *The Science*
- of the Total Environment, 869(161770), 161770. doi:10.1016/j.scitotenv.2023.161770
- 31. Ross, M. S., Loutan, A., Groeneveld, T., Molenaar, D., Kroetch, K., Bujaczek, T., ...
- Ruecker, N. J. (2023). Estimated discharge of microplastics via urban stormwater during
- individual rain events. Frontiers in Environmental Science, 11.
- 545 doi:10.3389/fenvs.2023.1090267
- 32. Sang, W., Chen, Z., Mei, L., Hao, S., Zhan, C., Zhang, W. B., ... Liu, J. (2021). The
- abundance and characteristics of microplastics in rainwater pipelines in Wuhan, China.
- 548 The Science of the Total Environment, 755(Pt 2), 142606.
- 549 doi:10.1016/j.scitotenv.2020.142606

- 33. Shruti, V. C., Pérez-Guevara, F., Elizalde-Martínez, I., & Kutralam-Muniasamy, G.
- 551 (2021). Current trends and analytical methods for evaluation of microplastics in
- stormwater. Trends in Environmental Analytical Chemistry, 30(e00123), e00123.
- 553 doi:10.1016/j.teac.2021.e00123
- 34. Smyth, K., Drake, J., Li, Y., Rochman, C., Van Seters, T., & Passeport, E. (2021).
- Bioretention cells remove microplastics from urban stormwater. *Water Research*,
- 556 191(116785), 116785. doi:10.1016/j.watres.2020.116785
- 35. Sun, X., Jia, Q., Ye, J., Zhu, Y., Song, Z., Guo, Y., & Chen, H. (2023). Real-time
- variabilities in microplastic abundance and characteristics of urban surface runoff and
- sewer overflow in wet weather as impacted by land use and storm factors. *The Science of*
- the Total Environment, 859(Pt 2), 160148. doi:10.1016/j.scitotenv.2022.160148
- 36. Sutton, Rebecca, Amy Franz, Alicia Gillbreath, Diana Lin, Liz Miller, Carolynn Box,
- Rusty Holleman, Keenan Munno, Xia Zhu, and Chelsea Rochman. 2019. *Understanding*
- 563 microplastic levels, pathways, and transport in the San Francisco Bay Region, 5 Gyres.
- Accessed January 12, 2024
- 37. Wayman, C., & Niemann, H. (2021). The fate of plastic in the ocean environment a
- minireview. Environmental Science. Processes & Impacts, 23(2), 198–212.
- 567 doi:10.1039/d0em00446d
- 38. Wei, L., Yue, Q., Chen, G., & Wang, J. (2023). Microplastics in rainwater/stormwater
- environments: Influencing factors, sources, transport, fate, and removal techniques.
- 570 Trends in Analytical Chemistry: TRAC, (117147), 117147.
- 571 doi:10.1016/j.trac.2023.117147

- 39. Werbowski, L. M., Gilbreath, A. N., Munno, K., Zhu, X., Grbic, J., Wu, T., ... Rochman,
- 573 C. M. (2021). Urban stormwater runoff: A major pathway for anthropogenic particles,
- black rubbery fragments, and other types of microplastics to urban receiving waters. ACS
- 575 ES&T Water, 1(6), 1420–1428. doi:10.1021/acsestwater.1c00017
- 576 40. Xue, W., Maung, G. Y. T., Otiti, J., & Tabucanon, A. S. (2023). Land use-based
- characterization and source apportionment of microplastics in urban storm runoffs in a
- tropical region. *Environmental Pollution*, 329, 121698.
- 579 doi:10.1016/j.envpol.2023.121698
- 41. Yano, K. A., Geronimo, F. K., Reyes, N. J., & Kim, L. H. (2021). Characterization and
- comparison of microplastic occurrence in point and non-point pollution sources. *The*
- *Science of the Total Environment*, 797(148939), 148939.
- 583 doi:10.1016/j.scitotenv.2021.148939
- 42. Yurtsever, M. (2021). Are nonwoven fabrics used in foods made of cellulose or plastic?
- Cellulose/plastic separation by using Schweizer's reagent and analysis based on a sample
- of tea bags. Process Safety and Environmental Protection: Transactions of the Institution
- 587 of Chemical Engineers, Part B, 151, 188–194. doi:10.1016/j.psep.2021.05.016
- 43. Zhou, L., Shen, G., Li, C., Chen, T., Li, S., & Brown, R. (2021). Impacts of land covers
- on stormwater runoff and urban development: A land use and parcel-based regression
- approach. Land Use Policy, 103(105280), 105280. doi:10.1016/j.landusepol.2021.105280
- 44. Ziajahromi, S., Drapper, D., Hornbuckle, A., Rintoul, L., & Leusch, F. D. L. (2020).
- Microplastic pollution in a stormwater floating treatment wetland: Detection of tire
- particles in sediment. The Science of the Total Environment, 713(136356), 136356.
- 594 doi:10.1016/j.scitotenv.2019.136356